# Multi-level memory-switching properties of a single brain microtubule

Satyajit Sahu, Subrata Ghosh, Kazuto Hirata, Daisuke Fujita, and Anirban Bandyopadhyay

Citation: Applied Physics Letters **102**, 123701 (2013); doi: 10.1063/1.4793995
View online: http://dx.doi.org/10.1063/1.4793995
View Table of Contents: http://scitation.aip.org/content/aip/journal/apl/102/12?ver=pdfcov
Published by the AIP Publishing

**Articles you may be interested in**

Resistive switching behaviors of Au/pentacene/Si-nanowire arrays/heavily doped n-type Si devices for memory applications
Appl. Phys. Lett. **104**, 053501 (2014); 10.1063/1.4863830

Scaling behaviors for resistive memory switching in NiO nanowire devices
Appl. Phys. Lett. **104**, 023513 (2014); 10.1063/1.4862751

Two-bit multi-level phase change random access memory with a triple phase change material stack structure
J. Appl. Phys. **112**, 104504 (2012); 10.1063/1.4765742

Multi-level phase change memory devices with Ge2Sb2Te5 layers separated by a thermal insulating Ta2O5 barrier layer
J. Appl. Phys. **110**, 124517 (2011); 10.1063/1.3672448

Nonvolatile multilevel memory effect by resistive switching in manganite thin films
J. Appl. Phys. **104**, 123705 (2008); 10.1063/1.3043801


This article is copyrighted as indicated in the article. Reuse of AIP content is subject to the terms at: http://scitation.aip.org/termsconditions. Downloaded to IP: 68.71.162.166 On: Thu, 27 Mar 2014 07:29:02

# Multi-level memory-switching properties of a single brain microtubule

Satyajit Sahu,[1] Subrata Ghosh,[1] Kazuto Hirata,[2] Daisuke Fujita,[1] and Anirban Bandyopadhyay[1,a)]
[1]*Advanced Nano Characterization Center, 1-2-1 Sengen, Tsukuba, Ibaraki 305-0047, Japan*
[2]*Superconducting Materials Center, National Institute for Materials Science, 1-2-1 Sengen, Tsukuba, Ibaraki 305-0047, Japan*

(Received 31 October 2012; accepted 18 February 2013; published online 26 March 2013)

We demonstrate that a single brain-neuron-extracted microtubule is a memory-switching element, whose hysteresis loss is nearly zero. Our study shows how a memory-state forms in the nanowire and how its protein arrangement symmetry is related to the conducting-state written in the device, thus, enabling it to store and process ~500 distinct bits, with 2 pA resolution between 1 nA and 1 pA. Its random access memory is an analogue of flash memory switch used in a computer chip. Using scanning tunneling microscope imaging, we demonstrate how single proteins behave inside the nanowire when this 3.5 billion years old nanowire processes memory-bits. © *2013 American Institute of Physics*. [http://dx.doi.org/10.1063/1.4793995]

Hysteresis is the backbone of an electronic-switching device, currently undergoing extensive structural and conceptual evolution to meet the challenges in the forthcoming era of complexity science.[1] If the embedded structure switches between two distinct symmetries, then, the device stores only two conducting states, 0 and 1, similar to the flash memory-devices used in the computer chip.[2] Multi-level switching devices[3–7] are the ne2wcomers that are structurally evolved to reversibly switch between multiple structural symmetries; yet, they are extremely slow in terms of operating speed. The concept of processing multiple bits in a single memory device can revolutionize the electronics industry.[8–10] First, it alleviates the limitations of binary system;[10] using these devices, we can implement multi-valued logic, which enables computerization of complex bio-inspired algorithms more efficiently.[9] Second, multi-layered complex neural network based problems could be studied. Third, extremely large data processing density could be achieved.

The most critical problem associated with memory-switching devices is the hysteresis loss, this is defined as the switching region in a perfect square current voltage (*IV*) characteristic. The "S" shaped *IV* loop that are frequently reported in the literatures as memory-device cannot be used in the futuristic chip, because enormous hysteresis loss would ensure massive heat production. The goal for constructing a perfect hysteresis loop has been a key concern for both the material scientists and the device engineers. The second problem is the mechanism for embedding multiple conducting states in a single memory-switching device. The hitherto adopted protocols[8–10] include, increased doping, multilayered architectures, composition of multiple redox-active materials, etc. These protocols are limited in implementation since establishment of one-to-one correspondence between carrier transmission and structural symmetry; tuning them during construction of multi-level switching devices is not addressed yet.

Here, we demonstrate that the symmetry of the dipoles have one to one correspondence with the multilevel conducting states of a microtubule,[11–13] directly with the scanning tunneling microscope (STM) imaging and measuring the conductivity of a single microtubule nanowire. Therefore, we demonstrate one of the fundamental origins of multilevel bit processing in a complex protein based architecture. We demonstrate live how dipolar orientation of the single tubulin protein dimer in the microtubule could be related to the conducting state of the microtubule. We report statistical analysis of the ac and dc conductivities of a single microtubule nanowire and demonstrate how a single microtubule device is compatible to a CMOS chip for ultra-fast rapid multi-level bit firing capacities.

Figure 1(a) shows tubulin protein and the protein made microtubule, a 25 nm wide and 200 nm to 25 $\mu$m long nanowire that appeared in the living cell for a mysterious reason, nearly 3.5 million years back. A single tubulin protein in this nanowire could store 14 electrons[13] and undergo dipolar switching by $\pm 23°$. Since the nanowire is made of folded 2D sheet of tubulin protein,[12] this nanowire has the potential to tune its proteins dipole moment direction to control the global conducting state. In the STM characterization of single tubulin protein and the microtubule nanowire, we observe that the conductivity of a single protein molecule falls beyond certain positive bias (see Figure 1(b)), while conductivity of a single microtubule shows a sharp peak at −20 mV (Figure 1(c)).

We dropped microtubule solution on a pre-prepared chip and with atomic force microscope (AFM) tip, and we measured surface conductivity of a single microtubule, using AFM tip as one electrode and the Pt-pad as the other. The AFM tip was 5 nm and measurement frequency was 1 MHz and 500 kHz; we found that surface conductivity remains constant, and a linear current voltage characteristic is observed as shown in Figure 2(a). We have used a special chip as shown in Figure 2(b) to orient the microtubule and make device using a single nanowire. Microtubule is synthesized by standard protocol described elsewhere.[11] In addition, the chip has several 200 nm gaps to capture storage of

a)Author to whom correspondence should be addressed. Electronic addresses: anirban.bandyo@gmail.com and anirban.bandyopadhyay@nims.go.jp.

 © 2013 American Institute of Physics

This article is copyrighted as indicated in the article. Reuse of AIP content is subject to the terms at: http://scitation.aip.org/termsconditions. Downloaded to IP: 68.71.162.166 On: Thu, 27 Mar 2014 07:29:02

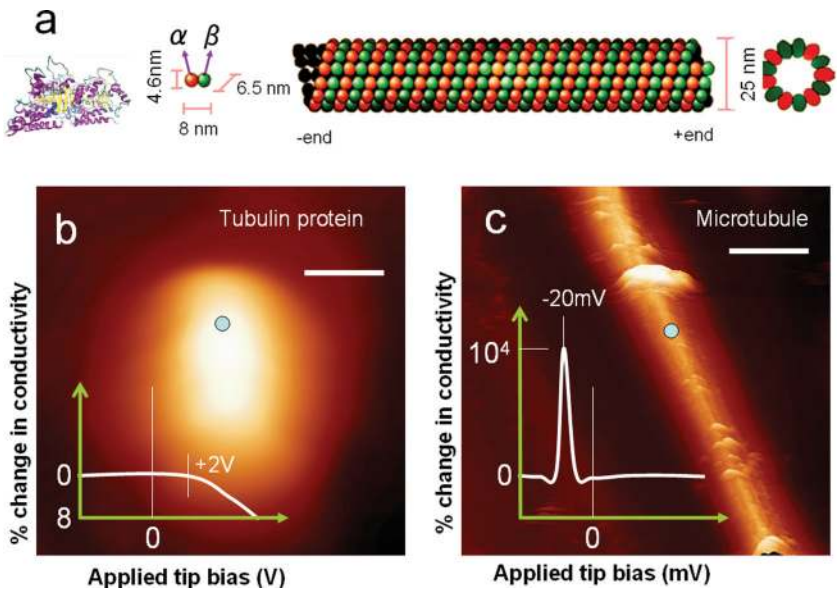


FIG. 1. (a) Tubulin protein dimer structure (left). A schematic showing dimensions of tubulin dimer and how 2D sheet of tubulin dimers fold into a single microtubule (middle). A schematic of cross-section of microtubule, STM measures conductivity across this ring. (b) STM image of a single tubulin dimer, tip bias 2 V, 100 pA, and scale bar is 4.3 nm. Inset shows percentage change in conductivity, as function of bias, from a typical current voltage characteristic measured on a point shown with a circle pointing on the top of the tubulin dimer. (c) STM image of a single microtubule, bias 2.7 V, 30 pA, and scale bar is 50 nm. Inset shows a similar plot like tubulin in panel (b).

ions, salts, and other impurities when microtubules grow and orient from single protein dimers. Afterwards, we take this chip and grow four 200 nm wide parallel gold electrodes on top of a single microtubule via e-beam lithography method (Fig. 2(c)) and measure the ac and dc conductivities of the device at different biases.

When we change the bias, the device ac and dc conductivities do not remain constant, rather, change with bias in a quantized manner (Figure 2(d)). In addition to bias, we have also changed the devices to see the variations of conductivities of various microtubules. Statistically, we observe two classes of microtubules as it is already seen with transmission electron microscope;[14] one has dc conductivities corresponding to the resistances in the range 1–10 MΩ and another, 300 MΩ. The measurement is done in air, open ambient atmosphere, and there was no change in the conductivity when we measured them in the ultra high vacuum condition. The ac conductivity of the first type goes down to a few kΩ, while the other goes down to a few hundreds of ∼kΩ. We have shown pie charts in Figures 2(e) and 2(f) to demonstrate these statistical analyses to summarize the observation in more than 100 s of microtubule devices studied over a period of four years.

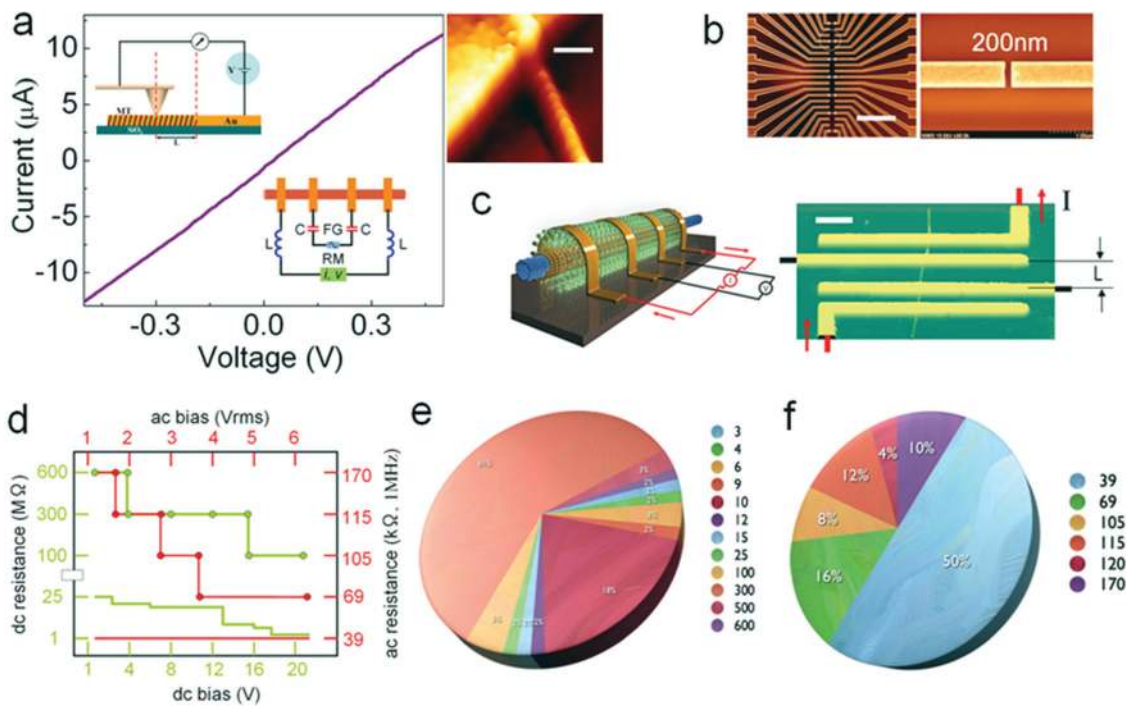


FIG. 2. (a) Current voltage characteristic along the surface of microtubule measured using AFM tip vibrating at 1 MHz, measurement circuit is shown at the top left panel and the corresponding AFM image is in the top right corner. The ac conductivity measurement circuit is at the right bottom inset. (b) The gold electrode chip on $Si/SiO_2$ substrate, scanning electron micrograph image, scale bar is 100 $\mu$m, the 200 nm wide ion trap region is zoomed. (c) Schematic of dc conductivity measurement set up (left), and AFM image of the device constructed, here current source is shown, for voltage source measurement only one pair of electrode was used. Scale bar is 400 nm. L is the actual device length. (d) The ac (red) and dc (green) resistance measurements in two typical devices, one class A (circle-line), another class B (line) as a function of applied bias. (e) Statistical distribution for dc resistances for 100 devices in Mega-Ohm. (f) Statistical distribution of ac resistances for 100 devices, at 1 MHz, in kilo-Ohm.

This article is copyrighted as indicated in the article. Reuse of AIP content is subject to the terms at: http://scitation.aip.org/termsconditions. Downloaded to IP: 68.71.162.166 On: Thu, 27 Mar 2014 07:29:02

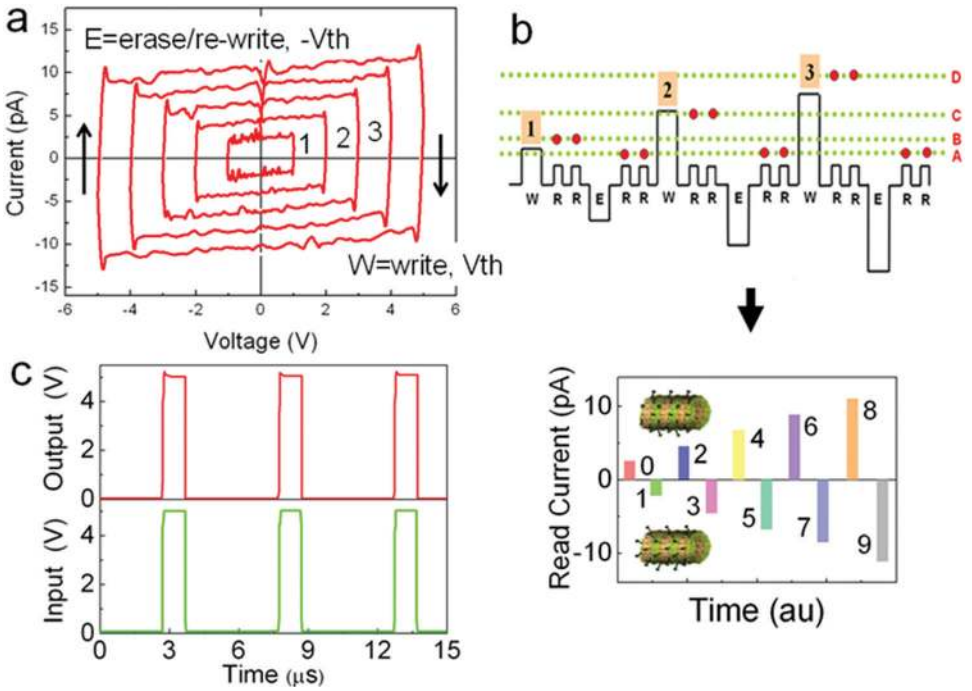


FIG. 3. (a) Five *IV* characteristics, using source voltage scan, the scan starts from 0 to $+V_{max}$ to $-V_{max}$ and then back $-V_{max}$ to $+V_{max}$, during scanning, $V_{max}$ was varied at a gap of 0.5 V from 0.5 V to 4.5 V bias, 1, 2, 3, 4, 5 volt data are shown. (b) (Top) Schematic of "write (W)—read (R)—erase(E)—read (R)" test-sequence for random access memory (RAM) and read only memory (ROM) applications, "1," "2," and "3" denotes writing pulses. (Below) 10 memory states were written varying from 1 mV to 90 mV and read using 0.1 mV read bias, only "read" currents (shown as A, B, C, D in b) are plotted here, 10 different currents probe 10 bits of memory-storage and processing. Read pulse and current has opposite polarity because "E" is not erase for microtubule, it is writing another state. (c) Using function generator we send stream of rectangular pulses (input, green) to a single microtubule device varying frequency 1 MHz to 20 GHz (repetition rate of the unit stream shown in b), output (red) is measured across 50 Ω resistance as voltage drop.

When we scan the bias $-V_{max}$ to $+V_{max}$ and then back to $-V_{max}$, we observe a nearly perfect square current voltage characteristic here in Figure 3(a). The hysteresis area is a function of maximum bias scan. From the current voltage characteristic, which moves clockwise (suggesting a hysteresis due to injected carriers, anti-clockwise hysteresis is observed with source current), we find that at a particular bias, the conductivity of the single microtubule nanowire increases or decreases suddenly, and we call this as the threshold bias for switching. To understand the memory storage and switching capabilities of a single microtubule device, we send a write-read-erase-read[15] signal as shown in Figure 3(b) (top), and the output is shown (below). Here, one multilevel memory state is written with an applied bias and erased by applying a reverse bias; the read bias is the same always. We send stream of short pulses across the single microtubule to find that the current grows and decays in less than a few nano-seconds (Figure 3(c)). Microtubule switches to the new conducting state as fast as the switches used in the computer chips. In conventional memory-switching devices, after erasing, we always get one single zero state, but here it is not, erasing is never a neutral state, rather a new conducting state.

This unique feature prompts us to correlate the dipole arrangement with the electric field. We replicate the

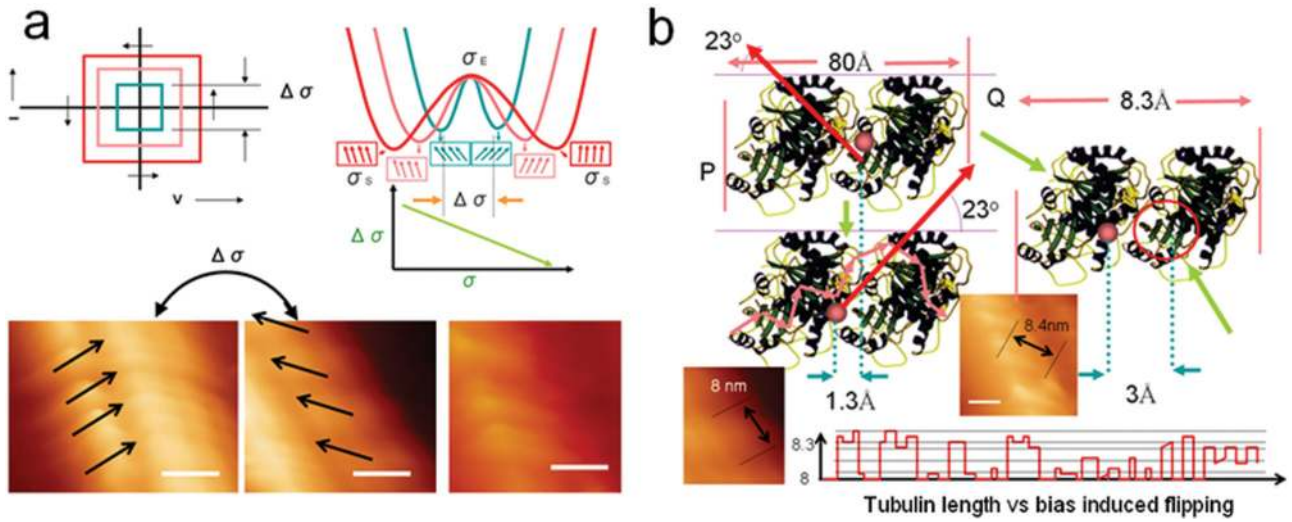


FIG. 4. (a) Schematic of square hysteresis current-voltage (*IV*) loop (top left), two nearly linear current-output regions depict a pair of memory-states, say top one is $+\sigma_S$ then bottom one is $-\sigma_S$, the corresponding conductivity difference between these two states is $\Delta\sigma$. Corresponding potential wells for $\pm\sigma_S$ are shown schematically (top right above), if $+\sigma_S$ is left well, $-\sigma_S$ is right well, $\sigma_E$ is the dip between two wells, since $\sigma_E$ signifies conductivity of microtubule with zero dipole-shift from original structure, and it is same for any memory-state-pair, we suggest it as $\sigma$. From Figure 3(a), a scheme is created by plotting $\Delta\sigma$ vs $\sigma$ (top right below). Three STM images with scale bar 6 nm, dipole direction shifts by a very small angle as shown with arrows. The arrows are plotted by scanning the region by changing STM rotation angle 0° to 180° at a gap of 10° and checking the high contrast regions on a single tubulin (bottom). (b) Tubulin structural parameters, gap between two monomers 0.13 nm to 0.3 nm, and we flip the bias to see that tubulin dimension changes in 5 different ways (5 memory bits), tubulins accommodate themselves on the surface as scan-bias changes.

This article is copyrighted as indicated in the article. Reuse of AIP content is subject to the terms at: http://scitation.aip.org/termsconditions. Downloaded to IP: 68.71.162.166 On: Thu, 27 Mar 2014 07:29:02

hysteresis-memory observed in the device measurement while visualizing the single microtubule inside the STM chamber. We vary the STM tip bias during scanning a proto-filament (linear chain of tubulin proteins on the microtubule surface) to find that the orientation of tubulin changes with an applied bias (Figure 4(a)). For particular orientations, the proto-filaments appear brighter, then, the tubulins are not distinctly visible, suggesting an increase in the longitudinal conductivity. When we write a conducting state of a single microtubule by scanning a small region of microtubule using STM tip, the flipping in the STM image contrast inside a single tubulin protein for the applied tip biases $\pm 3$ V (Figure 4(a) bottom) shows how the charge center of a single tubulin shifts by 0.3 nm, which increases its length and changes the orientation as shown in Figure 4(b). The connecting line between the high and the low contrast regions inside a single tubulin determines the dipole direction; these two contrast points flip similarly in an isolated tubulin and in the tubulin of a single microtubule. Finally, we show in Figure 4(b) below, how 5 bits are processed using STM-induced dipolar flipping. The plot suggests that the flipping is sufficient to generate distinct conducting states of a microtubule. Therefore, the arrangement of dipolar direction as shown with an arrow on tubulins at the microtubule surface STM image tells us in a single brain microtubule how a multi-level state is born and how it survives.

The theories often correlate dipoles with the memory-states of microtubule;[16–18] we have made the initial try to establish the one-to-one correspondence experimentally. This is not the complete evidence to establish the fundamental correlation; however, it marks the beginning for establishing such a correspondence.

Authors acknowledge Eiichiro Watanabe and Daiju Tsuya of Nanotechnology Innovation Station, NIMS Sengen-site Nano-oundry sponsored by Ministry of Science, Education, Culture and Sports (MEXT), Govt. of Japan. The current research work was funded by Asian office of Aerospace R&D, Govt. of USA FA2386-11-1-0001AOARD104173 and FA2386-10-1-4059 AOARD-10-4059.

There is no competing financial interest among the authors.

A.B. designed research; S.S. designed and built the microtubule device; S.S., A.B, K.H., and S.G, performed the experiments; A.B. and S.S. analyzed the data; A.B. wrote the paper; and D.F. reviewed the work.

[1]C. T. Butts, Science **325**(5939), 414–416 (2009).
[2]D. B. Strukov, G. S. Snider, D. R. Stewart, and R. S. Williams, Nature **453**(7191), 80–83 (2008).
[3]A. Bandyopadhyay, K. Miki, and Y. Wakayama, Appl. Phys. Lett. **89**(24), 243506–243509 (2006).
[4]V. Iancu and S. W. Hla, Proc. Natl. Acad. Sci. U.S.A. **103**(37), 13718–13721 (2006).
[5]N. S. Lee, H. K. Shin, and Y. S. Kwon, Jpn. J. Appl. Phys. **45**, 426 (2006).
[6]B. Simic Glavasky, "Molecular electro-optical transistor and switch," U.S. patent 4,804,930 (14 February 1989).
[7]B. Simic Glavasky, "Molecular architecture for molecular electro-optical transistor and switch," U.S. patent 7,136,212 (14 November 2006).
[8]R. Franke, F. J. Theis, and S. Klamt, J. Integr. Bioinform. **7**(1), 151–170 (2010).
[9]K. C. Smith, IEEE Trans. Comput. **C-30**(9), 619–634 (1981).
[10]V. V. Zhirnov, R. K. Cavin III, J. A. Hutchby, and G. I. Bourianoff, Proc. IEEE **91**(11), 1934–1939 (2003).
[11]D. K. Fygenson, E. Braun, and A. Libchaber, Phys. Rev. E **50**(2), 1579 (1994).
[12]J. R. McIntosh, M. K. Morphew, P. M. Grissom, S. P. Gilbert, and A. Hoenger, J. Mol. Biol. **394**(2), 177–182 (2009).
[13]I. Minoura and E. Muto, Biophys. J. **90**(10), 3739–3748 (2006).
[14]M. Kikkawa, T. Ishikawa, T. Nakata, T. Wakabayashi, and N. Hirokawa, J. Cell Biol. **127**(6), 1965–1971 (1994).
[15]A. Bandyopadhyay and A. J. Pal, Adv. Mater. **15**(22), 1949–1952 (2003).
[16]J. Brown and J. Tuszynski, Ferroelectrics **220**(1), 141–155 (1999).
[17]M. Satarić and J. Tuszyński, Phys. Rev. E **67**(1), 011901 (2003).
[18]J. Tuszyński, S. Hameroff, M. Satarić, B. Trpisova, and M. Nip, J. Theor. Biol. **174**(4), 371–380 (1995).

This article is copyrighted as indicated in the article. Reuse of AIP content is subject to the terms at: http://scitation.aip.org/termsconditions. Downloaded to IP: 68.71.162.166 On: Thu, 27 Mar 2014 07:29:02